Available online at www.sciencedirect.com
ScienceDirect
Geochimica et Cosmochimica Acta 71 (2007) 2402–2413
Geochimica et Cosmochimica Acta
www.elsevier.com/locate/gca

Osmium isotope systematics of ureilites

K. Rankenburg [a,b,*], A.D. Brandon [b], M. Humayun [a]

[a] National High Magnetic Field Laboratory, Department of Geological Sciences, Florida State University, Tallahassee, FL 32310, USA
[b] NASA Johnson Space Center, Mail Code KR, Houston, TX 77058, USA

Received 14 July 2006; accepted in revised form 21 February 2007; available online 25 February 2007

Abstract

The $^{187}Os/^{188}Os$ for 22 ureilite whole rock samples, including monomict, augite-bearing, and polymict lithologies, were examined in order to constrain the provenance and subsequent magmatic processing of the ureilite parent body (or bodies). The Re/Os ratios of most ureilites show evidence for a recent disturbance, probably related to Re mobility during weathering, and no meaningful chronological information can be extracted from the present data set. The ureilite $^{187}Os/^{188}Os$ ratios span a range from 0.11739 to 0.13018, with an average of 0.1258 ± 0.0023 (1σ), similar to typical carbonaceous chondrites, and distinct from ordinary or enstatite chondrites. The similar mean of $^{187}Os/^{188}Os$ measured for the ureilites and carbonaceous chondrites suggests that the ureilite parent body probably formed within the same region of the solar nebula as carbonaceous chondrites. From the narrow range of the $^{187}Os/^{188}Os$ distribution in ureilite meteorites it is further concluded that Re was not significantly fractionated from Os during planetary differentiation and was not lost along with the missing ureilitic melt component. The lack of large Re/Os fractionations requires that Re/Os partitioning was controlled by a metal phase, and thus metal had to be stable throughout the interval of magmatic processing on the ureilite parent body.

1. INTRODUCTION

The ureilites represent the second largest group among the achondritic meteorites, comprising ~16% of all achondrites. As of May 2006, the Meteoritical Bulletin database listed about 200 individual ureilite samples, some of which may be paired. Ureilites are best known as a distinct class of achondrites that appear to be products of a significant degree of planetary igneous differentiation, but also preserve primordial signatures that distinguishes them from other achondrite groups. Unlike other achondrite groups, the ureilites do not fall on a mass-dependent isotopic fractionation trend in oxygen isotope space (Clayton and Mayeda, 1988, 1996), but rather fall along a slope ~1 line defined by carbonaceous chondrite anhydrous minerals (CCAM). Ureilites also exhibit ^{33}S isotope anomalies (Farquhar et al., 2000), as well as large differences in $\delta^{15}N$ between ureilitic diamond, graphite, and silicate phases (Rai et al., 2003a). These isotopic heterogeneities are thought to preserve the primordial nebular heterogeneity in the accreting ureilite precursor materials and thus argue against a global magmatic equilibration of the ureilite parent body. Another apparently nebular signature that seems to preclude the significant outgassing that is expected from extensive magmatic processing is the high abundance of fractionated primordial noble gases that reside mostly in diamond (Göbel et al., 1977; Begemann and Ott, 1983; Rai et al., 2003b).

Petrographically, the monomict ureilites consist predominantly of olivine, pyroxene (mostly pigeonite, but also orthopyroxene and augite) and ⩽10% dark interstitial material consisting of carbon polymorphs (graphite, diamond, lonsdaleite, chaoite), metal, sulfides, and fine grained silicates (Goodrich, 1992; Mittlefehldt et al., 1998; Mittlefehldt, 2003; Goodrich et al., 2004). This material also occurs as veins that intrude the silicates along fractures and cleavage planes. With carbon abundances up to 6–7 wt%, the ureilites are the most carbon-rich meteorite group (Grady and Wright, 2003). On the basis of their silicate mineralogy, the monomict ureilites are classified into

* Corresponding author.
E-mail address: Rankenburg@magnet.fsu.edu (K. Rankenburg).

0016-7037/$ - see front matter © 2007 Elsevier Ltd. All rights reserved.
doi:10.1016/j.gca.2007.02.015

three different types: olivine-pigeonite, olivine-orthopyroxene, and augite-bearing. Succinct descriptions of the classification of monomict ureilites are given in Goodrich et al. (2004, 2006). Most monomict ureilites show coarse-grained igneous textures with mineral grains joining in abundant 120° triple junctions. Equilibration temperatures for ureilites estimated from two-pyroxene thermometry range from ~1200° to 1280 °C (Takeda, 1987; Takeda et al., 1989; Chikami et al., 1995; Sinha et al., 1997), whereas olivine-pigeonite-liquid thermometry (Singletary and Grove, 2003) suggests a slightly broader range from ~1150 to 1300 °C. Monomict ureilites lack plagioclase and are depleted in incompatible lithophile elements. In these respects the ureilites resemble typical terrestrial ultramafic upper mantle rocks (such as lherzolites and harzburgites) that experienced removal of a basaltic component during partial melting events.

The two main origins that have been considered for ureilites are as partial melting residues (Warren and Kallemeyn, 1992; Scott et al., 1993), or as cumulates (Berkley et al., 1976; Berkley and Keil, 1980; Berkley and Jones, 1982). Although most workers now accept the theory that ureilites are residues rather than cumulates, the augite-bearing ureilites, which represent a small percentage of all ureilites, are likely to be cumulates or paracumulates (Goodrich et al., 2004). The olivine and pyroxene core mg# [molar Mg/(Mg + Fe)] of the monomict ureilites as a whole have been proposed to be genetically linked via pressure-dependent carbon redox control (Berkley and Jones, 1982; Goodrich et al., 1987a;Walker and Grove, 1993; Sinha et al., 1997; Singletary and Grove, 2003, 2006). In this 'smelting' model, silicate FeO reacts with carbon in the presence of a silicate melt to form Fe-metal and carbon monoxide. A rapid, CO-gas driven localized melt extraction and loss of the melt into space resulting from high eruption velocities could provide an explanation for the lack of basaltic ureilites in the meteorite collections (Warren and Kallemeyn, 1992; Keil and Wilson, 1993; Scott et al., 1993). One problem of the smelting models is that they imply the loss of a significant amount of metallic iron in the more 'smelted', i.e., MgO-rich ureilites (Mittlefehldt, 2005; Warren and Huber, 2006). The high abundances and chondritic interelement ratios of several highly siderophile (iron-loving) elements (HSE—Ru, Rh, Pd, Re, Os, Ir, Pt, and Au) (Wänke et al., 1972; Boynton et al., 1976; Higuchi et al., 1976; Janssens et al., 1987; Mittlefehldt, 2005; Warren et al., 2006), however, are inconsistent with extensive removal of Fe-metal (as expected from the smelting model, or the segregation of a metallic core) because the metal would also effectively scavenge the siderophile elements from the rock.

In this paper, the Re–Os isotope system is used to address open questions in ureilite research. One question concerns the provenance of the ureilite protolith material. A basic tool for distinguishing between different meteorite classes is a categorization based upon their oxygen isotope composition (Clayton, 2003). Although ureilites do not have a 1:1 match with any known chondrite parent body (Clayton and Mayeda, 1996), they plot along an extension of the CV field on the CCAM line, partly overlapping with oxygen isotope data for the CR chondrites (Weisberg et al., 2001). Recently, it has been shown that there are significant differences in the $^{187}Re/^{188}Os$ and $^{187}Os/^{188}Os$ of carbonaceous chondrites compared with ordinary and enstatite chondrites (Walker et al., 2002). Therefore, the Os isotopic compositions may prove useful for 'fingerprinting' the provenance of planetesimals.

The Re–Os system is further explored in order to determine whether Re–Os chronology can provide additional constraints on the timing of ureilite differentiation. Available Sm–Nd and U–Pb ages for monomict ureilites are compatible with an early (~4.56 Ga) differentiation of the ureilite parent body (Goodrich and Lugmair, 1995; Torigoye-Kita et al., 1995b,c). A Pb–Pb age (4.56 ± 0.03 Ga) consistent with this was obtained from apatite from the polymict ureilite DaG 319 (Kita et al., 2002). Preliminary ^{182}Hf–^{182}W data for 8 monomict ureilites suggests an old age for these ureilites comparable to the timescales for differentiation of the howardite–eucrite–diogenite parent body, i.e. within a few million years since solar system formation (Lee et al., 2005). More recent high-precision Mg isotope analyses (Baker and Bizzarro, 2005) suggest extremely ancient model ages for the ureilites from potentially older than the calcium–aluminum-rich inclusions (CAIs – commonly thought to represent the oldest solids that formed in our solar system) to about 0.5 Ma after CAI formation. Polymict ureilites also contain Mn- and Al-rich clasts that yield ages of −4.5 ± 0.4 Ma relative to angrites using the ^{53}Mn–^{53}Cr short-lived radionuclide system (Goodrich et al., 2002), and ~5 Ma after formation of CAIs using the ^{26}Al–^{26}Mg system (Kita et al., 2003). Both methods yield a similar absolute age of ~4.562 Ga for these clasts, and hence, assuming that these clasts represent indigenous ureilitic lithologies, an estimate for the last magmatic activity on the ureilite parent body. However, some subsequent isotopic disturbance of ureilites is indicated by the most recent times of Ar degassing that have been inferred as 4.5–4.6 Ga for PCA 82506, but 4.1 Ga for Kenna and 3.3–3.7 Ga for Novo-Urei (Bogard and Garrison, 1994). In addition, it has been suggested for Kenna and Novo-Urei that material enriched in the light rare earth elements (LREE) was mobilized on the ureilite parent body at that time, possibly by impact (Goodrich et al., 1991; Goodrich and Lugmair, 1995), although it has also been argued that the 3.79 Ga Sm–Nd isochron for the ureilites Kenna, Novo-Urei, ALHA 77257 and Goalpara represents a mixing line due to terrestrial contamination (Torigoye-Kita et al., 1995a,b).

Natural Re is comprised of two isotopes, ^{185}Re (37.40 at.%) and ^{187}Re (62.60 at.%). The isotope ^{187}Re decays by β^- emission to ^{187}Os with a half-life of 41.6 Ga (Shen et al., 1996; Smoliar et al., 1996). Within the past 20 years, the ^{187}Re–^{187}Os system has established its rank among the radiogenic isotope systems commonly applied to cosmochemical issues (Shirey and Walker, 1998). Because Re and Os are both refractory and siderophile elements, the Re–Os system has proven useful in studies of primitive solar system materials such as the iron meteorites (Shen et al., 1996; Smoliar et al., 1996), but also CAIs and chondrites (Becker et al., 2001; Walker et al., 2002; Brandon et al., 2005a,b). Because the ureilites contain significant

amounts of metal, a Re–Os study seems appropriate to shed some light on their formation history.

2. SAMPLES

Twenty-two ureilites were analyzed in this study, including 16 Antarctic samples provided by the Astromaterials and Research Exploration Science Directorate at NASA-JSC (Table 1). Dyalpur (Field Museum of Natural History, Chicago), Jalanash (Institut für Planetologie, Münster) and Novo-Urei (National Museum of Natural History, Washington, USNM 2969) are observed falls from India, Mongolia and Russia, respectively. Goalpara (USNM 5992) and Kenna (USNM 5825) were found in India and the US, respectively. DaG 319, found in the Libyan Desert, was purchased for this study. The sample suite spans a broad compositional range representative of the ureilite group as a whole. Most of the ureilites in this study have typical monomict olivine-pigeonite lithologies. In the initial thin section description of EET 96042 no pyroxene was observed (Satterwhite and Lindstrom, 1998), whereas another study lists this ureilite as pigeonite-bearing (Cloutis and Hudon, 2004). MET 01085 has been described as olivine-free (Satterwhite and Allen, 2002); it is however, like all ureilites, sufficiently coarse-grained to provide the possibility that other sections of MET 01085 do contain olivine. LEW 85440, META 78008 and ALH 82130 (paired with ALH 82106, not analyzed) are augite-bearing. LEW 88774 is augite-bearing and also notable for being one of only two ureilites known to contain primary chromite. DaG 319 is the only polymict ureilite analyzed in this study. Weathering categories A, B, and C (Table 1) are used by the Meteorite Working Group at the NASA Johnson Space Center in Houston for Antarctic meteorite finds, denoting minor, moderate, and severe rustiness of hand specimens. Weathering levels of the analyzed ureilites vary from very fresh (including the falls) to severely rusty (LEW 86216). The warm-desert sample DaG 319 is classified as W2, meaning moderate oxidation of metal, 20–60% being affected (Wlotzka, 1993). Shock levels for the ureilites are taken from the compilation given in Mittlefehldt et al. (1998).

3. ANALYTICAL TECHNIQUES

All sample preparation and chemistry was performed at the Johnson Space Center. Initial sample masses ranged from 75 mg (LEW 86216) to 5.2 g (GRA 98032). Most of the ureilite samples were coarsely crushed to mm-sized pieces using a ceramic alumina mortar and pestle. Three of the largest samples (DaG 319: 5 g; Goalpara: 3 g; Kenna: 4.5 g) were crushed to a fine powder. Between samples, the mortar and pestle were cleaned by grinding quartz sand in ethanol to a fine powder, and then boiled in hot dilute nitric acid, followed by multiple rinses with Milli-Q ultra-pure water. Approximately 20–30 mg of rock chips (usually in 1–4 pieces) were handpicked from the coarsely crushed samples. If the outer rind of the meteorite was part of the original sample chip, material from the interior was taken for analyses. Leaching of the samples in dilute acids to reduce the effects of weathering in the Antarctic environment was not performed, because this could remove iron oxides (which likely contain Re and Os) in more strongly weathered samples. One sample (LEW 86216) showed very strong alteration in the form of pervasive iron oxides throughout the sample. In this case, the optically freshest parts were used for analysis, biasing the LEW 86216 analysis towards the iron oxide-poor side. To investigate sample reproducibility, sample GRA 98032 (total sample mass 5.2 g, weathering level C) was analyzed three times. A subsample of 90 mg rock chips was ground to a fine powder. Two ~20 mg subsamples of GRA 98032 were taken from this 90 mg powdered aliquot, another ~20 mg subsample was taken from the remaining rock chips (Table 1).

Sample digestion followed established procedures (Shirey and Walker, 1995). The rock chips or powders (~20 mg) were loaded in quartz Carius tubes, followed by addition of 2 ml concentrated HCl and a mixed spike enriched in ^{185}Re and ^{190}Os (Brandon et al., 2005a). The mixtures were then frozen in a dry-ice/ethanol slush before adding 4 ml of concentrated HNO_3 resulting in a reverse aqua regia solution. The Carius tubes were then sealed and heated in an oven for 72 h at 230 °C. The Carius tube digestion method is effective at dissolving metal and reaching spike-sample equilibration (Walker et al., 2002), but it is not a total dissolution method for silicate-bearing rocks. However, olivine and pyroxene are strongly attacked during the digestion procedure and the ureilite silicate rock matrix completely disintegrated. Moreover, the bulk of ureilite HSE are hosted in interstitial metal phases (Janssens et al., 1987) and the high-temperature igneous processing of ureilites precludes the occurrence of highly refractory primordial HSE-bearing alloys as observed for example in CAIs (Becker et al., 2001), or other refractory phases as observed in unequilibrated bulk chondrites (Brandon et al., 2005b). After digestion, Os was extracted from the reverse aqua regia using carbon tetrachloride solvent, then back extracted into HBr (Cohen and Waters, 1996), and finally purified by microdistillation (Birck et al., 1997). Following Os extraction, the aqua regia solutions were dried down and converted into chloride form, dissolved in 0.15 N HCl, and loaded onto cation exchange columns for Re separation and purification (Puchtel and Humayun, 2001).

Osmium cuts were loaded onto Pt filaments with a mixed NaOH–$Ba(OH)_2$ emitter. The concentrations and isotopic compositions reported in Table 1 were measured at the Johnson Space Center by negative ion thermal ionization mass spectrometry (N-TIMS) using a Thermo Finnigan Triton in static multicollection mode. Oxygen corrections were made using the oxygen isotope composition measured on 2 ng loads of ReO_4^- on the Faraday cups. The O_2 pressures in the source were maintained in the range of $1–3 \times 10^{-7}$ mbar for all runs. The ^{187}Re interference on ^{187}Os was monitored at mass 233 $^{185}Re^{16}O_3^-$ and was not observed during any of the sample measurements. After oxygen corrections were performed on the raw data, instrumental mass fractionation was corrected using $^{192}Os/^{188}Os = 3.083$ and the exponential law. The Johnson–Matthey Os isotope standard gave $^{187}Os/^{188}Os = 0.11380 \pm 1$ (2σ) during the analytical period, identical to

Table 1
Re and Os concentrations and Os isotopic ratios for ureilites

Ureilite	Mineral ass.			Weath. level	Shock level	Weight (mg)	ol core (Fo)	Re m. (ppb)	2σ (%)	Re c. (ppb)	Os (ppb)	$^{187}Re/^{188}Os$ (ppb)	$^{187}Re/^{188}Os$ meas.	$^{187}Os/^{188}Os$ calc.	±2σ
ALH 82130	+aug	Chips	Find	B	Medium	26.40	94.9	15	0.5	13	165	0.4246	0.3816	0.12545	2
ALHA 77257	ol-pig	Chips	Find	Ae	Low	24.06	87.1	9.2	0.6	10	118	0.3771	0.3892	0.12604	2
ALHA 78019	ol-pig	Chips	Find	B/C	Very low	16.82	76.7	64	0.4	98	1195	0.2576	0.3946	0.12647	1
ALHA 81101	ol-pig	Chips	Find	A/B	High	17.90		2.2	0.8	2.9	43	0.2498	0.3294	0.12132	9
ALHA 81101	dupl.[a]	Chips				73.93	78.5	1.9	0.8	1.9	34	0.2717	0.2796	0.11739	8
DaG 319	polymict	Powder	Find	W2	Low	17.48		10	2.3	18	226	0.2202	0.3893	0.12605	1
DaG 319	dupl.[a]	Powder				50.24		11	1.2	19	234	0.2220	0.3933	0.12637	20
Dyalpur	ol-pig	Chips	Fall	(A)	High	23.87	84.3	20	1.2	24	295	0.3199	0.3875	0.12591	3
EET 87517	ol-pig	Chips	Find	B/C	Low	21.18	92.3	18	0.4	25	322	0.2748	0.3722	0.12470	2
EET 96042	ol(-pig)	Chips	Find	A/B	Medium	19.80	82.0	34	0.4	26	318	0.5098	0.3906	0.12616	2
EET 96042	dupl.[a]	Chips				40.03		32	0.8	35	441	0.3479	0.3876	0.12592	1
Goalpara	ol-pig	Powder	Find	(A)	High	16.12	78.6	8.8	0.6	8.7	109	0.3913	0.3843	0.12566	8
Goalpara	dupl.[a]	Powder				81.06		8.9	1.8	8.5	107	0.3987	0.3836	0.12560	8
GRA 95205	ol-pig	Chips	Find	B	High	18.82	79.1	74	0.3	74	869	0.4112	0.4113	0.12779	17
GRA 95205	dupl.[a]	Chips				61.84		58	0.5	68	791	0.3533	0.4168	0.12822	1
GRA 98032	ol-pig	Powder	Find	C	High	17.31	75.0	42	0.3	26	314	0.6374	0.4035	0.12717	1
GRA 98032	dupl.	Powder				19.42		29	0.3	26	308	0.4583	0.4026	0.12710	1
GRA 98032	dupl.	Chips				22.18		21	0.3	27	319	0.3240	0.4010	0.12698	1
GRO 95575	ol-pig	Chips	Find	A/B	Low	23.38	78.7	25	0.5	18	218	0.5419	0.3900	0.12611	1
Jalanash	ol-pig	Chips	Fall	(A)	S3	14.40	81.0	12	0.6	13	163	0.3684	0.3886	0.12600	6
Kenna	ol-pig	Powder	Find	(B)	Medium	19.45	78.9	34	0.6	42	504	0.3211	0.3981	0.12675	2
Kenna	dupl.[a]	Powder				21.01		32	0.7	40	476	0.3217	0.4021	0.12706	28
LEW 85328	ol-pig	Chips	Find	B/C	Low	22.00		3.2	0.6	3.5	48	0.3224	0.3562	0.12344	9
LEW 85328	dupl.[a]	Chips				51.74	80.0	7.3	0.9	7.6	98	0.3613	0.3726	0.12473	5
LEW 85440	+aug	Chips	Find	B	Low	57.68	91.0	14	1.2	19	236	0.2823	0.3854	0.12574	3
LEW 86216	ol-pig	Chips	Find	C	High	27.96	80.6	13	0.7	46	563	0.1082	0.3927	0.12632	5
LEW 88774	chromite	Chips	Find	B/C	Medium	14.72	74.9	26	2.4	36	431	0.2907	0.4055	0.12733	9
MET 01085	opx (+ol?)	Chips	Find	B	Medium	28.91	*90*	18	0.5	19	282	0.3146	0.3270	0.12113	2
META 78008	+aug	Chips	Find	B	Medium	20.04	77.0	66	0.6	98	1071	0.2957	0.4416	0.13018	1
Novo-Urei	ol-pig	Chips	Fall	(A)	Medium	24.79	78.9	28	0.4	29	351	0.3807	0.3979	0.12673	4
PCA 82506	ol-pig	Chips	Find	A/Be	Low	18.03	79.0	21	0.4	27	328	0.3052	0.3942	0.12644	4

n.m., not measured; Re m., measured Re concentrations from ID-ICP-MS; Re c., Re concentrations calculated from Os concentrations and Os isotopic ratios assuming an age of 4562 Ma. 2σ-errors of $_{187}Os/_{188}Os$ refer to the last digits given. 2σ-errors for Os concentrations from ID-TIMS analyses are estimated to be better than 0.1%. Olivine Fo of sample MET 01085 is estimated from a olivine–pyroxene correlation in ureilites as a whole (Mittlefehldt et al., 1998). Weathering grades in parenthesis are estimated from petrographic descriptions. Prefixes of Antarctic samples: ALH, Allan Hills; LEW, Lewis Cliff; PCA, Pecora Escarpment; EET, Elephant Moraine; GRO, Grosvenor Mountains; GRA, Graves Nunataks; MET, Meteorite Hills.

[a] Duplicates acquired in a second session.

previously published values (Brandon et al., 1999; Brandon et al., 2005a,b).

The Re isotopic compositions were measured on a Finnigan Element™ single-collector, magnetic sector, high-resolution ICP-MS at the National High Magnetic Field Laboratory using an ESI™ PFA spray chamber and an ESI™ 100 μl/min nebulizer (Puchtel and Humayun, 2001). The samples were run alternately with matrix solution blanks and a standard solution of similar Re concentration to the sample solutions. Instrumental mass fractionation was corrected by normalizing the measured $^{185}Re/^{187}Re$ used for isotope dilution (ID) calculations with a mass fractionation factor obtained by comparing the measured $^{185}Re/^{187}Re$ in the standard solution to the natural value (0.5974). For the majority of samples, the internal precision of individual ID-ICP-MS runs for the determination of Re concentrations (Table 1) had uncertainties of $0.54 \pm 0.34\%$ (2σ, $n = 25$, Table 1). For 5 samples (Dyalpur, Goalpara, LEW 88774, LEW 85440, DaG 319) the Re chemistry yields were low, resulting in larger errors on $^{187}Re/^{185}Re$ of 1.2 to 2.4% (Table 1). Total external uncertainties (2σ) for Os concentrations from ID-TIMS analyses are estimated to be better than 0.1%. The total analytical blanks ranged between 2 and 22 (average 8) pg Re, and between 0.2 to 3.7 (average 1.4) pg Os. Blank corrections on sample Re concentrations averaged 2%, but were 11 and 18% for the samples LEW 85328 and ALHA 81101 that have very low Re abundances. Blank corrections on sample Os concentrations were <0.1%. Because samples ALHA 81101 and LEW 85328 were also largely overspiked during a first set of measurements, these samples were subsequently duplicated along with two other samples from a fresh dissolution of a larger (40–70 mg) subsample of the coarse rock chips left from initial sample crushing (i.e., ALHA 81101, EET 96042, GRA 95205, and LEW 85328, cf. Table 1). The spiked Re cuts of three additional duplicates of homogenized sample powders (DaG 319, Goalpara, and Kenna) have been split for parallel N-TIMS determinations. Because N-TIMS analyses resulted in slightly lower uncertainties of calculated Re concentrations, these data are reported for the DaG 319, Goalpara and Kenna duplicates in Table 1.

4. RESULTS

Measured Re abundances for the studied ureilites range from ~0.1 times CI (Horan et al., 2003) in ALHA 81101 to ~2 times CI in ALHA 78019, whereas Os abundances in the same ureilites range from ~0.1 times CI to ~2.6 times CI (Table 1). Compared to previous Re–Os data from neutron activation analysis for the same ureilites (Warren et al., 2006), the Re concentrations deviate between −60% (ALHA 81101) to +48% (PCA 82506), and Os deviates from −34% (Novo-Urei) to +164% (META 78008) from the literature values, respectively. Sample sizes in previous studies ranged between 100 and 500 mg, whereas sample sizes in this study ranged mostly between 20 and 30 mg (Table 1), but also included three large (3–5 g) homogenized samples. It is not the intention of this study to determine absolute Re and Os abundances in ureilites, and 20 mg fractions of ureilites may not be representative of the whole meteorites. Even Kenna (4.5 g of homogenized powder) differs from the literature Os concentration value (Warren et al., 2006) by 30% in this study. Considering that allocated sample masses are usually much smaller than 4.5 g, and that many ureilite meteorites have less than 4.5 g of total mass, it seems that absolute trace element abundances in ureilites will generally remain afflicted with considerable uncertainty.

The external reproducibilities of Re and Os concentration measurements for 20 mg aliquots taken from the large (3–5 g) powdered samples Goalpara, DaG 319 and Kenna are within 1.1 and 1.9%, 4.6 and 3.5%, and 5.7 and 5.6%, respectively, and decrease with overall increasing Re–Os abundances in the samples (Fig. 1a). The reproducibility of the Re/Os ratio, however, increases with increasing Re–Os abundances, and is within 2.0, 0.6 and 0.2% for these samples, respectively. Three subsamples (powders and chips) of sample GRA 98032 showed virtually identical Os concentrations, but large Re abundance variations (Fig. 1a). Duplicate analyses of individual rock chip subsamples show more scatter with no obvious dependence on absolute Re–Os abundances, or weathering level (Fig. 1b).

The Os isotope analyses of all analyzed ureilites, including 9 duplicates, are reported in Table 1. The ureilite $^{187}Os/^{188}Os$ form a unimodal distribution, and range from 0.11739 to 0.13018, with a mean of 0.1258 ± 0.0023 (1σ) (Fig. 2). The polymict ureilite DaG 319, which contains feldspathic lithologies that may be derived from the missing

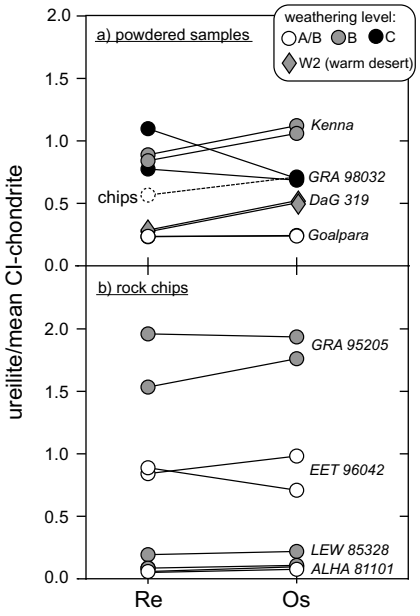

Fig. 1. External reproducibilities of Re and Os concentrations of 8 ureilites from 9 individual dissolutions. (a) Duplicates from larger masses of homogenized sample powders (Goalpara, DaG 319, Kenna: 3–5 g; GRA 98032: 90 mg). An independent analysis of GRA 98032 rock chips is indicated as dashed line. (b) Duplicates from small (~20 mg) subsamples of ureilite rock chips. Weathering levels cold-desert: A/B—open, B—grey, C—black dots; warm-desert: W2—triangles.

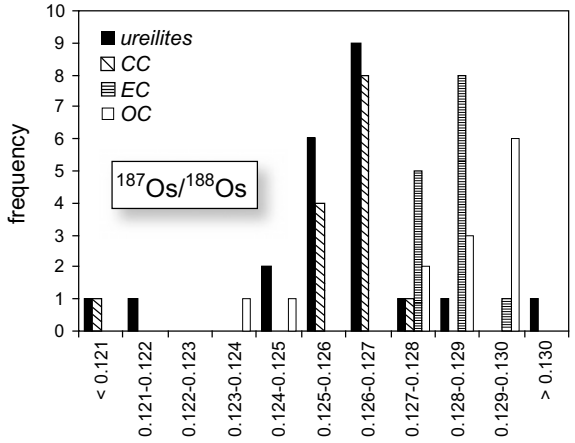

Fig. 2. Comparison of ureilite $^{187}Os/^{188}Os$ with different chondrite groups (Walker et al., 2002; Brandon et al., 2005a). CC, carbonaceous; EC, enstatite; OC, ordinary chondrites.

silicate melts from the ureilite parent body (Ikeda and Prinz, 2001; Cohen et al., 2004; Goodrich et al., 2004; Kita et al., 2004; Downes and Mittlefehldt, 2006), has $^{187}Os/^{188}Os$ of 0.1262 ± 0.0004 (2σ) indistinguishable from the monomict ureilite average [0.1257 ± 0.0024 (1σ)]. Inverse Os concentrations and Os isotopic compositions of the ureilites are ($r^2 = 0.66$) correlated (Fig. 3a). There are, however, no significant correlations of Os isotopic compositions with pyroxene (i.e., ureilite) type, olivine (Fig. 3b) or pyroxene (not shown) core compositions, shock level (Fig. 3c), modal pyroxene content, $\delta^{33}S$ (Fig. 3d), or $\Delta^{17}O$ (Fig. 3e).

5. DISCUSSION

5.1. Effects of terrestrial weathering on ureilite Re and Os abundances and Os isotopes

As pointed out in earlier work (Esser and Turekian, 1993; Peucker-Ehrenbrink and Blum, 1998; Brandon et al., 2000; Walker et al., 2002), terrestrial crustal materials typically have $^{187}Os/^{188}Os$ of $\geqslant 1$, and widely varying, very high Re/Os. However, because of the relatively high concentrations of Os in the ureilite samples of 50 – 1200 ppb (Table 1), combined with the low concentrations of Os in crustal rocks and minerals of <0.05 ppb, i.e., 1000–20,000 times less Os compared to the samples, it is highly unlikely that $^{187}Os/^{188}Os$ ratios were changed by Antarctic weathering. This is also consistent with a recent study on the weathering behavior of CK carbonaceous chondrites (Huber et al., 2006) where even severely weathered Antarctic samples showed no resolvable anomaly in their Os abundance compared to other CK finds and falls. Re was not measured in the latter study; it is, however, expected to be more mobile during terrestrial weathering than other platinum group elements (Jaffe et al., 2002). The main Re and Os-bearing phase in ureilites is kamacite that is associated with carbonaceous material (Wänke et al., 1972; Wlotzka, 1972; Janssens et al., 1987). Fractionations in whole rock Re/Os

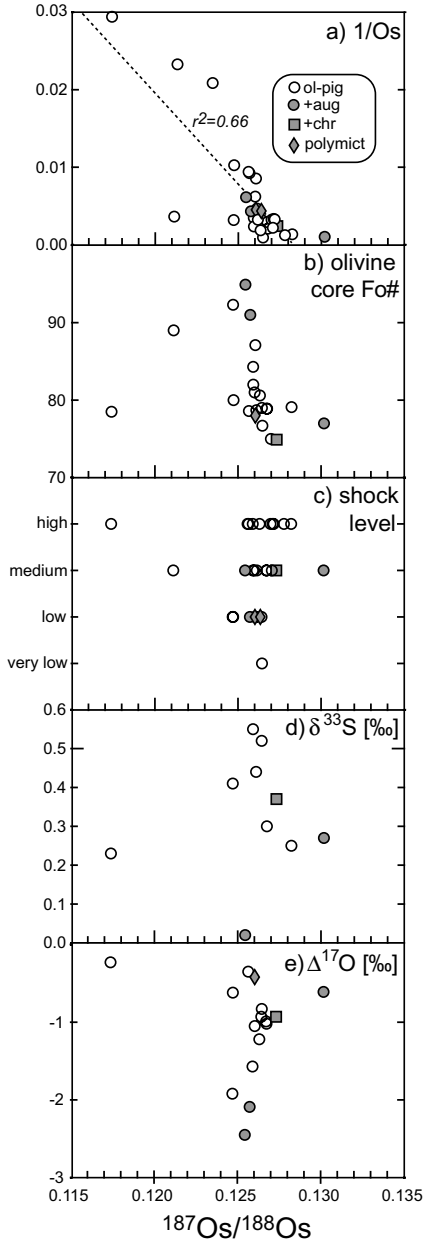

Fig. 3. $^{187}Os/^{188}Os$ of ureilites versus inverse Os concentrations (a), olivine forsterite contents (Fo) of silicate matrix (b), shock levels (c), $\delta^{33}S$ (d), and $\Delta^{17}O$ isotope compositions (e) (Clayton and Mayeda, 1988; Mittlefehldt et al., 1998; Farquhar et al., 2000).

should occur only if Re and Os, once weathered out of the metal via formation of hydrous Fe-oxides, show largely different mobility within their host rock.

To investigate the effects of weathering on Re and Os in the studied suite of ureilites, time averaged $^{187}Re/^{188}Os$ were calculated from the measured $^{187}Os/^{188}Os$ of the samples (Table 1) assuming a formation age of the ureilites of 4562 Ma (Torigoye-Kita et al., 1995c; Goodrich et al., 2002; Kita et al., 2003) and closed-system Re/Os evolution. From these ratios, and the measured Os concentrations, average time-integrated Re concentrations were calculated for each ureilite (Table 1), and are compared with the

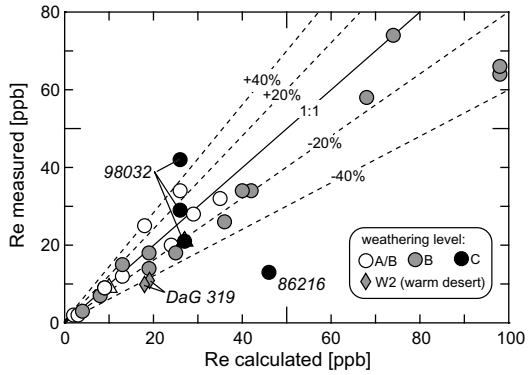

Fig. 4. Measured Re concentrations versus time-averaged Re concentrations inferred from Os isotopes in ureilites. Open triangles mark samples containing visible evaporite minerals. Polymict ureilite DaG 319 (filled triangles) is the only warm-desert sample.

measured Re concentrations (Fig. 4). The measured and calculated Re concentrations are correlated and scatter around a 1:1 reference line (Fig. 4). The visible evaporite minerals reported for two ureilites (weathering grade 'e', Table 1) do not seem to additionally disturb the Re–Os system. Correlation coefficients are similarly high among groups of samples classified as weathering grades A and B with $r^2 = 0.91$ and 0.94, respectively. In contrast, two samples classified as C (LEW 86216 and three duplicates of GRA 98032, Table 1) show large scatter ($r^2 = 0.31$). Two independent subsamples of GRA 98032 (chips and powder coming from different parts of the original sample slab) have consistent Os abundances within 3.5% of each other, but variable Re abundances (Fig. 1a), which can be interpreted as Re mobility, but Os immobility in the hydrous Antarctic environment. Furthermore, the discrepancy in Re concentration between the two powdered subsamples of GRA 98032 suggests that homogenization was not achieved during sample grinding for this sample. Re mobility is also indicated for the most strongly weathered sample LEW 86216 that shows the largest Re loss (−72%) (Fig. 4). Because pieces of LEW 86216 that showed major rustiness were avoided for analyses, it is concluded that Re was either preferentially transferred to the iron oxides (short-range redistribution), or removed from the sample (long-range redistribution). Long-range redistribution of Re is more consistent with the general Re loss indicated for the large homogenized sample Kenna (-19%) (Fig. 1a). The ureilites with intermediate and minor weathering grades span a range of measured Re concentrations from approximately −40% to +40% relative to their calculated Re concentrations (Fig. 4, Table 1). In comparison, the warm-desert sample DaG 319 (weathering level W2) lost 44% of its Re when compared to the calculated Re concentration from Os isotopes (Fig. 4).

The observed variability of Os concentrations in duplicate analyses of independent subsamples of ureilite rock chip (GRA 95205 and EET 96042, Fig. 1), and the much higher Os concentrations of samples GRA 95205 (+76%) and META 78008 (+164%) compared to previous data (Warren et al., 2006), are attributed to heterogeneous distribution of HSE-bearing metals within individual ureilite subsamples. A similar conclusion was made in studies of Os isotope/HSE systematics in chondrites (Walker et al., 2002; Horan et al., 2003). Very few Fe-metal abundances are reported for ureilites (Wiik, 1972; Jarosewich, 1990; Yanai and Noda, 2005). However, because of their variable distribution on the centimeter scale, Fe-metal abundances in a specific ureilite likely depend on the specific aliquot or thin section analyzed. In conclusion, absolute abundances of Os appear to be affected by heterogeneous distribution of metal, while those of Re have additionally been affected by weathering processes, both of which reduce the precision with which conclusions can be drawn from absolute Re and Os abundances about HSE distribution during ureilite petrogenesis. However, Os isotopes should be much less affected by such sample heterogeneity because even if metal was mobile in the ureilite parent body, the Re/Os and hence present-day $^{187}Os/^{188}Os$ isotopic composition of that metal should be fairly homogeneous.

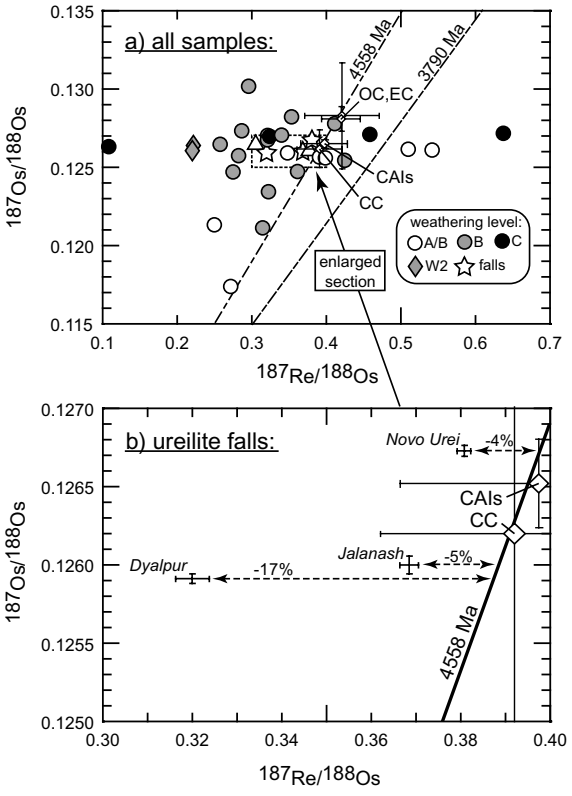

Fig. 5. (a) Re–Os isochron diagram for ureilite whole rocks, along with means and 2σ-intervals for the chondrite groups (Walker et al., 2002), and CAIs with unfractionated REE patterns (Chen et al., 1999; Becker et al., 2001). Shown for reference is the Group IIIA iron meteorite isochron with initial $^{187}Os/^{188}Os = 0.09524$ and slope 0.07887 that is assumed to represent an age of 4558 Ma (Smoliar et al., 1996), and a calculated 3790 Ma reference line. Most of the data lie on a zero-age isochron indicating recent Re mobilization, with strongly weathered samples (black dots) showing the widest overall spread in $^{187}Re/^{188}Os$. All error bars for ureilite samples are smaller than symbol size. (b) Re–Os isochron diagram for ureilite falls. Novo-Urei and Jalanash have similar Re–Os isotope compositions to carbonaceous chondrites, and plot close to the 4558 Ma reference isochron.

When plotted in a $^{187}Os/^{188}Os$ versus $^{187}Re/^{188}Os$ isochron diagram (Fig. 5a), most of the data scatter around a horizontal zero age isochron, consistent with recent mobilization and open system behavior of Re. There is no indication that $^{187}Re/^{188}Os$ or $^{187}Os/^{188}Os$ ratios of strongly weathered samples (weathering grade C) were preferentially shifted to superchondritic values, as would be expected from terrestrial contaminants. Because of the overall large scatter in ureilite Re/Os, however, no meaningful age information can be deduced from the whole rock data. Even when the dataset is restricted to the group of ureilite falls, no useful isochron can be fitted to the data because of the insufficient range in Re/Os. However, a subset of the ureilite whole rock data that includes the falls clusters more closely around the 4558 Ma Group IIIA iron meteorite reference isochron (Fig. 5a), and two of the three ureilite falls studied have a measured Re–Os isotope composition that is indistinguishable from that of carbonaceous chondrites (Walker et al., 2002). Argon isotopic data for the Kenna and Novo-Urei ureilites suggest disturbances of at ~4.1 Ga and 3.3–3.7 Ga (Bogard and Garrison, 1994), respectively, consistent with the suggested time of LREE-mobilization in these meteorites at ~3.79 Ga (Goodrich et al., 1991; Goodrich and Lugmair, 1995). Although the Re–Os data for Kenna is compromised by too large weathering effects for a reliable Re–Os age estimate, the fresh ureilite fall Novo-Urei plots close to the 4558 Ma reference isochron (Fig. 5b). Thus, whatever caused the argon isotopic disturbances in Novo-Urei did not produce a noticeable effect on the Re–Os isotope system.

5.2. The provenance of the ureilite parent body

5.2.1. Ureilite HSE systematics

Ureilite HSE budgets have been suggested to be a mixture of a refractory-rich component that is associated with the veins, and a refractory-poor component associated with the silicates (Wänke et al., 1972; Boynton et al., 1976; Higuchi et al., 1976; Janssens et al., 1987; Spitz and Boynton, 1991). Later work has shown that ureilite HSE abundance patterns are consistent with solid metal/liquid metal fractionation, indicating that residual metal is present in ureilites (Goodrich et al., 1987a,b; Janssens et al., 1987; Jones and Goodrich, 1989; Humayun et al., 2005; Warren and Huber, 2006; Warren et al., 2006). A good match for the siderophile element patterns of ureilites with high Re and Os abundances is obtained assuming that ureilites are residues of carbonaceous chondrite precursors after extraction of a S-rich (>15%) liquid metal component (Humayun et al., 2005). Osmium isotopes provide a means to test the hypothesis that these two components with low versus high Re and Os abundances are characterized by distinct Os isotopic compositions. Mixing of two isotopically distinct Os components should form a straight line in a 1/Os versus $^{187}Os/^{188}Os$ plot (Fig. 3b). Although the observed correlation is defined mainly by the two depleted samples ALHA 81101 and MET 01085 (Fig. 3a), elimination of these two samples in the calculation still yields a significant correlation (95.1% confidence) in the remaining data set. It can therefore be concluded that Os isotopes are consistent with mixing of an Os-poor component (probably associated with the silicates) with long-term depletion in Re/Os, and Os-rich residual metal that is associated with the carbonaceous material and has more carbonaceous chondrite-like Re/Os and consequent $^{187}Os/^{188}Os$ of ~0.1265 (Fig. 3a).

The mean and distribution of $^{187}Os/^{188}Os$ measured for the ureilites (0.1258 ± 0.0023) are similar to those measured in carbonaceous chondrites (0.1258 ± 0.0018) and in CAIs with relatively unfractionated REE patterns (0.1265 ± 0.0003), but different from those measured for ordinary chondrites (0.1281 ± 0.0020) or enstatite chondrites (0.1281 ± 0.0005). The polymict (brecciated) ureilites are composed of >98% material similar to the monomict ureilites (Goodrich et al., 2004; Downes and Mittlefehldt, 2006). These materials encompass an identical range of mineralogical compositions to that shown by all known monomict ureilites, and also show similar relative proportions of the different petrologic types. The $^{187}Os/^{188}Os$ of 0.1262 ± 0.0004 (2σ, ext.) measured in this study for the polymict ureilite DaG 319 is consistent with the average $^{187}Os/^{188}Os$ of the 21 monomict ureilites, and thus in agreement with the petrographic observations.

The division of bulk chondrites on the basis of $^{187}Os/^{188}Os$ into two groups (carbonaceous versus ordinary/enstatite chondrites) may result from differential high-temperature nebular condensation of Re and Os into refractory element-bearing alloys and their subsequent isolation and incorporation into the precursor materials of certain chondrite groups (Walker et al., 2002). Alternatively, the observed disparate Re/Os could also be a result of lower-temperature oxidation or heating loss of Re in the precursor materials of carbonaceous chondrite components (Walker et al., 2002). The overlapping $^{187}Os/^{188}Os$ for certain CAIs and carbonaceous chondrites, however, suggest a bulk solar system value of ~0.1265 (Becker et al., 2001), and the high-temperature condensation scenario therefore seems more plausible. In the following, two conclusions are derived from the similar distribution and mean of $^{187}Os/^{188}Os$ measured for ureilites and for carbonaceous chondrites (Fig. 2).

First, the similarly narrow range of $^{187}Os/^{188}Os$ (i.e., similar standard deviation) observed for ureilites and carbonaceous chondrites is taken as evidence that partial melting in the ureilite parent body, accumulation of metal, and different degrees of shock (Fig. 3c) early in ureilite petrogenesis did not lead to a significant fractionation of Re from Os. In particular, metallic iron (i.e., residual metal) must have been a stable phase in the early fractionation history, because in the absence of a metal phase, Re should behave incompatibly and may have been lost along with the missing ureilitic melt component. For example, if the ureilite precursor material experienced early magmatic processing above the iron-wuestite oxygen buffer, Re and Os partitioning would be expected to be comparable to melt extraction in the terrestrial upper mantle at similar oxygen fugacities. For example, Al_2O_3 contents correlate with $^{187}Os/^{188}Os$ in terrestrial orogenic lherzolites (Reisberg and Lorand, 1995). This relationship is consistent with similar incompatibilities and proportional removal of Al_2O_3 and Re from the peridotite residues during partial melting

in an oxidized, metal-free terrestrial upper mantle. Terrestrial peridotite xenoliths from the non-convecting subcontinental lithospheric mantle have lost on average 63% of their Re compared to the present fertile convecting mantle (Shirey and Walker, 1998). Compared to average CI and CV chondrites (Wasson and Kallemeyn, 1988), average ureilites (Warren et al., 2006) have lost 66 and 83% of their aluminum, respectively, similar to the terrestrial analogue. Assuming a chondritic starting composition at 4562 Ma and a relative proportion of Re equivalent to Al_2O_3 was lost (i.e., a present-day $^{187}Re/^{188}Os$ ranging between 0.0666 and 0.1333), then the present-day average $^{187}Os/^{188}Os$ for the ureilites should be $\leqslant 0.1058$. Because such low $^{187}Os/^{188}Os$ is not observed for the ureilites studied here, it is concluded that Re was not significantly lost relative to Al_2O_3 during melt extraction, and thus metal must have been a stable phase throughout ureilite magmatic processing. The presence of metal implies oxygen fugacities that were below the iron-wuestite oxygen buffer throughout the melting interval. It must be noted that some carbonaceous chondrites contain very little metal, and HSE may be concentrated in sulfides. Unlike ureilites, these carbonaceous chondrites did not undergo magmatic processing and melt removal, and therefore retained their bulk Re/Os.

Second, the similar mean of $^{187}Os/^{188}Os$ measured for the ureilites and carbonaceous chondrites suggests that the ureilite parent body probably formed within the same region of the solar nebula as carbonaceous chondrites. This conclusion from Os isotopes is supported by oxygen isotopes of ureilites (Clayton and Mayeda, 1996). In the oxygen three-isotope plot (Fig. 6), ureilites plot along an extension of the CCAM, but are clearly distinct from ordinary and enstatite chondrites. The reason for the slightly lower-than-average $^{187}Os/^{188}Os$ of ALHA 81101 and MET 01085 is unclear. While ALHA 81101 is a relatively unweathered, highly shocked, low forsterite (Fo), and pigeonite-poor ureilite characterized by the lowest overall Re and Os abundances measured in this study; MET 01085 is an unusual orthopyroxene-bearing ureilite with intermediate values for weathering grade, Re and Os abundances, Fo contents, and shock level (Table 1, Fig. 3a–c). Thus the low $^{187}Os/^{188}Os$ cannot be connected to any other petrologic feature, arguing against the presence of a distinct subchondritic $^{187}Os/^{188}Os$ and Os-poor component associated with the silicates as suggested from the correlation in Fig. 3a.

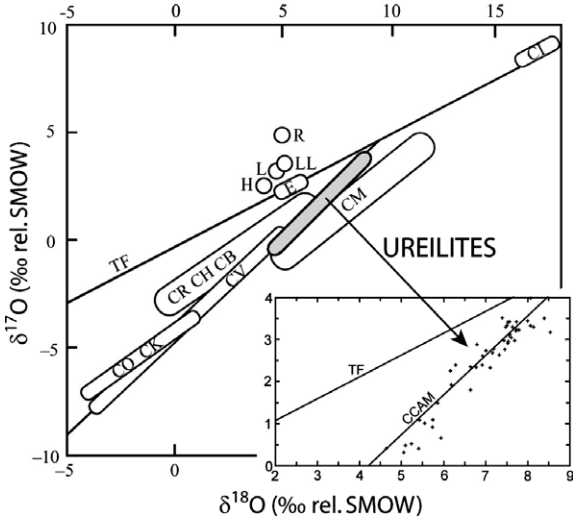

Fig. 6. Oxygen isotopes of ureilites compared to different chondrite groups. Adapted and modified from (Clayton and Mayeda, 1996) and (Clayton, 2003). The ureilites form a tight cluster around the carbonaceous chondrite anhydrous mineral (CCAM) line, and plot between CV3 matrix components and the intersection of the CCAM line with the terrestrial and CI chondrite mass fractionation line.

Subchondritic $^{187}Os/^{188}Os$ could in principle result from extraction of a S-rich metal phase from the ureilites. Solid metal/liquid metal distribution coefficients ($D^{SM}/_{LM}$) for Re and Os during such liquid metal extraction are dependent on the S-content of the liquid metal phase (Chabot and Jones, 2003; Chabot et al., 2003; Rushmer et al., 2005), which decreases during batch melting as a function of temperature from the eutectic composition (~30 wt% S in the liquid phase). Using the $D^{SM}/_{LM}$ parameterization of (Chabot and Jones, 2003), and assuming a simplified binary Fe–S system, $D^{SM}/_{LM}$ for Re and Os are in the order of several thousands at the Fe–S eutectic, but decrease to 34.9 and 36.9, respectively, for a liquid metal S-content of ~20 wt% that correspond to the peak metamorphic temperatures for the ureilites of 1300 °C. The liquid fraction F produced at the Fe–S eutectic is dependent on the initial FeS to Fe-metal ratio of the ureilite protolith, and the peak metamorphic temperature. However, for all melt fractions between 1% and 99%, and S-contents of the extracted melt between 0 and 30%, the calculated Re/Os fractionations in residual metal are always smaller than 1.66%; and a fractionation in Re/Os at 4562 Ma of this magnitude would lead to a present-day deficit in $^{187}Os/^{188}Os$ of the residual metal of 0.41%. It is concluded that extraction of a Fe–S liquid from the ureilites is unsuitable to explain the $^{187}Os/^{188}Os$ deficits of ALHA 81101 and MET 01085 of 6.6 and 3.7%, respectively, relative to the ureilite average (Table 1).

A low $^{187}Os/^{188}Os$ value [0.11980 ± 0.00004 (2σ)] similar to the two anomalous samples ALHA 81101 and MET 01085 has been measured for the undifferentiated CK4 chondrite Karoonda (Walker et al., 2002). This opens the possibility that the low $^{187}Os/^{188}Os$ of ALHA 81101 and MET 01085 might reflect heterogeneous carbonaceous chondritic precursor material.

5.2.2. What is the ureilite precursor material?

Ureilite Os isotope data are indistinguishable from those of carbonaceous chondrites, but a more specific assignment to a specific chondrite group is not possible with Os isotopes alone. In oxygen isotopes, ureilites do not have a 1:1 match with any carbonaceous chondrite parent body (Fig. 6). The ureilites plot along an extension of the CV field on the CCAM line, partly overlapping with oxygen data for the CR chondrites (Weisberg et al., 2001). The CCAM line may be explained as a mixing line between ^{16}O-rich

condensates from the unaltered primary nebular gas having approximately −45‰ for both $\delta^{17}O$ and $\delta^{18}O$, and material from the inner part of the accretion disk enriched in ^{17}O and ^{18}O by the photolysis of CO (Clayton, 2002). The large range in $\delta^{18}O$ of each carbonaceous chondrite group compared to the ordinary and enstatite groups (Fig. 6) is probably a result of low-temperature aqueous alteration, which produces phyllosilicates enriched in the heavy isotopes (Clayton and Mayeda, 1999). For example, the phyllosilicate matrix of CM and CO chondrites is systematically enriched in $\delta^{18}O$ and $\delta^{17}O$ relative to the whole rock, and the tie-lines between whole-rock compositions and matrix compositions have slopes of ~0.7. In the case of the CV chondrites, the large range in $\delta^{18}O$ may represent internal isotopic heterogeneity due to the presence of ^{16}O-rich refractory phases (Clayton and Mayeda, 1999). The offset between CV chondrites and ureilites on the CCAM thus could be explained if the ureilite protolith is similar to CV chondrites, but contained less refractory phases. The close fit of the ureilites to the CCAM line with slope ~1 can be taken to imply that aqueously altered carbonaceous chondrite material (CI, CM or CR) was at most a minor component of the ureilite parent body.

A CV-type precursor of the ureilites, however, is at odds with the carbon abundance in ureilites [0.7–6.6 wt%, average 2.9 wt% (Hudon et al., 2004; Mittlefehldt, 2005; Warren et al., 2006)], which is higher than that in CV chondrites by a factor of about 5, but comparable to CI and CR chondrites [averages 0.53, 3.45, and 2.0 wt%, respectively (Lodders and Fegley, 1998)]. The $\delta^{13}C$ isotopic compositions of ureilites range from −11 to +1‰ (Hudon et al., 2004), and are also more akin to CI than CV chondrites [$\delta^{13}C$ ranging from −12 to −5‰ and −25 to −8‰, respectively (Grady and Wright, 2003)]. Although the carbon isotopic composition of the ureilites might have been altered by magmatic processing (Hudon et al., 2004), magmatic models are difficult to reconcile with the observed carbon enrichment of ureilites compared to CV chondrites. For example, loss of 30% silicate melt from the precursor would passively increase the carbon content of CV-type material to 0.8 wt%, far below the observed average abundance in ureilites. Chromium isotope data for Kenna and LEW 85440 suggest that the initial Cr isotope ratios of ureilites are distinct from those of carbonaceous chondrites, but similar to the HED parent body (Shukolyukov and Lugmair, 2006; Trinquier et al., 2005). However, the origin of ^{54}Cr variation in the early solar system is as yet unclear and needs to be substantiated by further measurements. In conclusion, no known chondrite class seems to meet all the necessary conditions to provide a suitable ureilite precursor material. Nevertheless, oxygen and Os isotopes strongly suggest an affinity of ureilites to carbonaceous chondrites.

6. CONCLUSION

In conclusion, absolute abundances of Os in ureilites appear to be affected by heterogeneous distribution of metal, while those of Re have additionally been affected by weathering processes. Because of Re losses during weathering, no meaningful age information can be deduced from the ureilite whole rock data. However, a subset of the ureilite whole rock data that includes the falls clusters more closely around the 4558 Ma Group IIIA iron meteorite reference isochron, consistent with the old age of the ureilites obtained from other dating methods. From the similar mean and distribution of $^{187}Os/^{188}Os$ measured for the ureilites and carbonaceous chondrites it is concluded that the ureilite parent body probably formed within the same region of the solar nebula as carbonaceous chondrites. Partial melting in the ureilite parent body, accumulation of metal, and different degrees of shock early in ureilite petrogenesis did not lead to a significant fractionation of Re from Os. In particular, metallic iron (i.e., residual metal) must have been a stable phase throughout the early ureilite magmatic history.

ACKNOWLEDGMENTS

We are grateful to the Astromaterials and Research Exploration Science Directorate at NASA-JSC for providing the Antarctic ureilite samples. We thank Glenn MacPherson, Linda Schramm, and the U.S. National Museum of Natural History in Washington for samples of Goalpara, Kenna and Novo-Urei. We also thank the Field Museum in Chicago for samples of Dyalpur and Jalanash. The manuscript greatly benefited from comments made by N. Kita, C. Goodrich, P.H. Warren, and one anonymous reviewer. K.R. was supported by a post-doctoral research appointment at NASA managed by the National Research Council and Oak Ridge Associated Universities. This research was funded by the NASA Cosmochemistry program under grants RTOP 344-31-72-06 to ADB and NNG05GB81G to M.H.

REFERENCES

Baker J. A., and Bizzarro M. (2005) ^{26}Mg-deficit dating of differentiated meteorites with Al/Mg ~0: accretion and melting of proto-planets in the first million years of the solar system. In *Proc. Protostars Planets Conf.* **5**. #8612 (abstr.) [CD-ROM].

Becker H., Walker R. J., Macpherson C. G., Morgan J. W., and Grossman J. N. (2001) Rhenium–osmium systematics of calcium–aluminum-rich inclusions in carbonaceous chondrites. *Geochim. Cosmochim. Acta* **65**(19), 3379–3390.

Begemann F., and Ott U. (1983) Comment on "The nature and origin of ureilites" by J. L. Berkley et al. *Geochim. Cosmochim. Acta* **47**(5), 975–977.

Berkley J. L., and Jones J. H. (1982) Primary igneous carbon in ureilites—petrological implications. *J. Geophys. Res.* **87**, A353–A364.

Berkley J. L., and Keil K. (1980) Ureilites revisited—petrologic evidence for a cumulate origin. *Meteoritics* **15**(4), 264–265.

Berkley J. L., Brown I., Gassaway H., Keil K., Carter N. L., Mercier J.-C. C., and Huss G. (1976) The Kenna ureilite: an ultramafic rock with evidence for igneous, metamorphic, and shock origin. *Geochim. Cosmochim. Acta* **40**(12), 1429–1430.

Birck J. L., Roy-Barman M., and Capmas F. (1997) Re–Os isotopic measurements at the femtomole level in natural samples. *Geostand. Newsl.-J. Geostand. Geoanal.* **21**(1), 19–27.

Bogard D. D., and Garrison D. H. (1994) ^{39}Ar–^{40}Ar ages of four ureilites (abstr.). *Lunar Planet. Sci. Conf.* **25**(1), 137–138.

Boynton W. V., Starzyk P. M., and Schmitt R. A. (1976) Chemical evidence for the genesis of the ureilites, the achondrite Chassigny and the nakhlites. *Geochim. Cosmochim. Acta* **40**(12), 1439–1447.

Brandon A. D., Norman M. D., Walker R. J., and Morgan J. W. (1999) ^{186}Os–^{187}Os systematics of Hawaiian picrites. *Earth Planet. Sci. Lett.* **174**(1–2), 25–42.

Brandon A. D., Walker R. J., Morgan J. W., and Goles G. G. (2000) Re–Os isotopic evidence for early differentiation of the Martian mantle. *Geochim. Cosmochim. Acta* **64**(23), 4083–4095.

Brandon A. D., Humayun M., Puchtel I., and Zolensky M. E. (2005a) Re–Os isotopic systematics and platinum group element composition of the Tagish Lake carbonaceous chondrite. *Geochim. Cosmochim. Acta* **69**(6), 1619–1631.

Brandon A. D., Humayun M., Puchtel I. S., Leya I., and Zolensky M. (2005b) Osmium isotope evidence for an s-process carrier in primitive chondrites. *Science* **309**, 1233–1236.

Chabot N. L., and Jones J. H. (2003) The parameterization of solid metal-liquid metal partitioning of siderophile elements. *Meteorit. Planet. Sci.* **38**, 1425–1436.

Chabot N. L., Campbell A. J., Jones J. H., Humayun M., and Agee C. B. (2003) An experimental test of Henry's Law in solid metal–liquid metal systems with implications for iron meteorites. *Meteorit. Planet. Sci.* **38**, 181–196.

Chen J. H., Papanastassiou D. A., and Wasserburg G. J. (1999) Re–Os systematics in the Allende CAI: Big Al. *Lunar Planet. Sci. Conf.* **30**. #1483 (abstr.) [CD-ROM].

Chikami J., Mikouchi T., Miyamoto M., and Takeda H. (1995) Equilibration temperature of Lewis-Cliff-88774 and other ureilites (abstr.). *Meteoritics* **30**(5), 498.

Clayton R. N. (2002) Self-shielding in the solar nebula. *Nature* **415**, 860–861.

Clayton R. N. (2003) Oxygen Isotopes in Meteorites. In *Treatise on Geochemistry: Meteorites, Comets, and Planets* (ed. A.M. Davis). vol. 1, pp. 129–142. Elsevier.

Clayton R. N., and Mayeda T. K. (1988) Formation of ureilites by nebular processes. *Geochim. Cosmochim. Acta* **52**(5), 1313–1318.

Clayton R. N., and Mayeda T. K. (1996) Oxygen isotope studies of achondrites. *Geochim. Cosmochim. Acta* **60**(11), 1999–2017.

Clayton R. N., and Mayeda T. K. (1999) Oxygen isotope studies of carbonaceous chondrites. *Geochim. Cosmochim. Acta* **63**(13–14), 2089–2104.

Cloutis, E. A., and Hudon, P. (2004) Reflectance spectra of ureilites: Nature of the mafic silicate absorption features. *Lunar Planet. Sci. Conf.* **35**. #1257 (abstr.) [CD-ROM].

Cohen A. S., and Waters F. G. (1996) Separation of osmium from geologic materials by solvent extraction for analysis by TIMS. *Anal. Chim. Acta* **332**, 269–275.

Cohen B. A., Goodrich C. A., and Keil K. (2004) Feldspathic clast populations in polymict ureilites: stalking the missing basalts from the ureilite parent body. *Geochim. Cosmochim. Acta* **68**(20), 4249–4266.

Downes H. and Mittlefehldt D. W. (2006) Evidence for a single ureilite parent asteroid from a petrologic study of polymict ureilites. *Lunar Planet. Sci. Conf.* **37**. #1150 (abstr.) [CD-ROM].

Esser B. K., and Turekian K. K. (1993) The osmium isotopic composition of the continental crust. *Geochim. Cosmochim. Acta* **57**(13), 3093–3104.

Farquhar J., Jackson T. L., and Thiemens M. H. (2000) A ^{33}S enrichment in ureilite meteorites: evidence for a nebular sulfur component. *Geochim. Cosmochim. Acta* **64**(10), 1819–1825.

Göbel R., Ott U., and Begemann F. (1978) On trapped noble gases in ureilites. *J. Geophys. Res.* **83**, 855–867.

Goodrich C. A. (1992) Ureilites: a critical review. *Meteoritics* **27**(4), 327–352.

Goodrich C. A., and Lugmair G. W. (1995) Stalking the LREE-enriched component in ureilites. *Geochim. Cosmochim. Acta* **59**(12), 2609–2620.

Goodrich C. A., Jones J. H., and Berkley J. L. (1987a) Origin and evolution of the ureilite parent magmas: multi-stage igneous activity on a large parent body. *Geochim. Cosmochim. Acta* **51**(9), 2255–2273.

Goodrich C. A., Jones J. H., and Spitz A. H. (1987b) Siderophile element tests of ureilite petrogenesis models. *Meteoritics* **22**(4), 392–394.

Goodrich C. A., Patchett P. J., Lugmair G. W., and Drake M. J. (1991) Sm–Nd and Rb–Sr isotopic systematics of ureilites. *Geochim. Cosmochim. Acta* **55**(3), 829–848.

Goodrich C. A., Hutcheon I. D., and Keil K. (2002) ^{53}Mn-^{53}Cr age of a highly-evolved, igneous lithology in polymict ureilite DaG 165 (abstract). *Annual Meeting of the Meteoritical Society* **65**, #5190 [CD-ROM].

Goodrich C. A., Scott E. R. D., and Fioretti A. M. (2004) Ureilitic breccias: clues to the petrologic structure and impact disruption of the ureilite parent asteroid. *Chemie der Erde - Geochemistry* **64**(4), 283–327.

Goodrich C. A., Wlotzka F., Ross D. K., and Bartoschewitz R. (2006) Northwest Africa 1500: Plagioclase-bearing monomict ureilite or ungrouped achondrite? *Meteorit. Planet. Sci.* **41**(6), 925–952.

Grady M. M., and Wright I. P. (2003) Elemental and isotopic abundances of carbon and nitrogen in meteorites. *Space Sci. Rev.* **106**(1–4), 231–248.

Higuchi H., Morgan J. W., Ganapathy R., and Anders E. (1976) Chemical fractionations in meteorites X: ureilites. *Geochim. Cosmochim. Acta* **40**(12), 1563–1571.

Horan M. F., Walker R. J., Morgan J. W., Grossman J. N., and Rubin A. E. (2003) Highly siderophile elements in chondrites. *Chem. Geol.* **196**, 5–20.

Huber H., Rubin A. E., Kallemeyn G. W., and Wasson J. T. (2006) Siderophile-element anomalies in CK carbonaceous chondrites: Implications for parent-body aqueous alteration and terrestrial weathering of sulfides. *Geochim. Cosmochim. Acta* **70**(15), 4019–4037.

Hudon P., Romanek C., Paddock L., and Mittlefehldt D. W. (2004) Evolution of the ureilite parent body. *Lunar Planet. Sci. Conf.* **35**. #2075 (abstr.) [CD-ROM].

Humayun, M., Rushmer, T., Rankenburg, K., and Brandon, A. D. (2005) A model for siderophile element distribution in planetary differentiation. *Lunar Planet. Sci. Conf.* **36**. #2208 (abstr.) [CD-ROM].

Ikeda Y., and Prinz M. (2001) Magmatic inclusions and felsic clasts in the Dar al Gani 319 polymict ureilite. *Meteorit. Planet. Sci.* **36**(4), 481–499.

Jaffe L. A., Peucker-Ehrenbrink B., and Petsch S. T. (2002) Mobility of rhenium, platinum group elements and organic carbon during black shale weathering. *Earth Planet. Sci. Lett.* **198**(3–4), 339–353.

Janssens M. J., Hertogen J., Wolf R., Ebihara M., and Anders E. (1987) Ureilites: trace element clues to their origin. *Geochim. Cosmochim. Acta* **51**(9), 2275–2283.

Jarosewich E. (1990) Chemical analyses of meteorites: a compilation of stony and iron meteorite analyses. *Meteoritics* **25**, 323–337.

Jones J. H., and Goodrich C. A. (1989) Siderophile trace-element partitioning in the Fe–Ni–C system—preliminary-results with application to ureilite petrogenesis. *Meteoritics* **24**(4), 281–282.

Keil K., and Wilson L. (1993) Explosive volcanism and the compositions of cores of differentiated asteroids. *Earth Planet. Sci. Lett.* **117**, 111–124.

Kita N. T., Ikeda Y., and Morishita Y. (2002) The old Pb–Pb age of apatite in felsic clast of polymict ureilite DaG 319 (abstr.). *Meteorit. Planet. Sci.* **37**(7), A79.

Kita N. T., Ikeda Y., Togashi S., Shimoda G., Morishita Y., and Weisberg M. K. (2003) Evolution of ureilites by Al-26 heating

of the parent body (abstr.). *Geochim. Cosmochim. Acta* **67**(18), A220.

Kita N. T., Ikeda Y., Togashi S., Liu Y., Morishita Y., and Weisberg M. K. (2004) Origin of ureilites inferred from a SIMS oxygen isotopic and trace element study of clasts in the Dar al Gani 319 polymict ureilite. *Geochim. Cosmochim. Acta* **68**(20), 4213–4235.

Lee D. -C., Halliday A. N., Singletary S. J., and Grove T. L. (2005) ^{182}Hf–^{182}W chronometry and an early differentiation on the parent body of ureilites. *Lunar Planet. Sci. Conf.* **36**. #1638 (abstr.) [CD-ROM].

Lodders K., and Fegley B. (1998) *The Planetary Scientist's Companion*. Oxford University Press.

Mittlefehldt D. W. (2003) Achondrites. In *Treatise on Geochemistry: Meteorites, Comets, and Planets*, vol. 1 (ed. A.M. Davis). Elsevier, pp. 291–324.

Mittlefehldt D. W., Hudon P., and Galindo, Jr., C. (2005) Petrology, geochemistry and genesis of ureilites. *Lunar Planet. Sci. Conf.* **36**. #1040 (abstr.) [CD-ROM].

Mittlefehldt D. W., McCoy T. J., Goodrich C. A., and Kracher A. (1998) Non-chondritic meteorites from asteroidal bodies. In *Planetary Material*, vol. RIM 36 (ed. J. J. Papike). The Mineralogical Society of America, pp. 4.1–4.195.

Peucker-Ehrenbrink B., and Blum J. D. (1998) Re–Os isotope systematics and weathering of Precambrian crustal rocks: Implications for the marine osmium isotope record. *Geochim. Cosmochim. Acta* **62**(19–20), 3193–3203.

Puchtel I., and Humayun M. (2001) Platinum group element fractionation in a komatiitic basalt lava lake. *Geochim. Cosmochim. Acta* **65**, 2979–2993.

Rai V. K., Murty S. V. S., and Ott U. (2003a) Nitrogen components in ureilites. *Geochim. Cosmochim. Acta* **67**(12), 2213–2237.

Rai V. K., Murty S. V. S., and Ott U. (2003b) Noble gases in ureilites: cosmogenic, radiogenic, and trapped components. *Geochim. Cosmochim. Acta* **67**(22), 4435–4456.

Reisberg L., and Lorand J. P. (1995) Longevity of subcontinental mantle lithosphere from osmium isotope systematics. *Nature* **376**, 159–162.

Rushmer T., Petford N., Humayun M., and Campbell A. J. (2005) Fe-liquid segregation in deforming planetesimals: Coupling Core-Forming compositions with transport phenomena. *Earth Planet. Sci. Lett.* **239**(3–4), 185–202.

Satterwhite C., and Allen C. (2002). *Antarctic Meteorite Newsl.* **25**(2), 15.

Satterwhite C., and Lindstrom M. (1998). *Antarctic Meteorite Newsl.* **21**(1).

Scott E. R. D., Taylor G. J., and Keil K. (1993) Origin of Ureilite Meteorites and Implications For Planetary Accretion. *Geophys. Res. Lett.* **20**(6), 415–418.

Shen J. J., Papanastassiou D. A., and Wasserburg G. J. (1996) Precise Re–Os determinations and systematics of iron meteorites. *Geochim. Cosmochim. Acta* **60**(15), 2887–2900.

Shirey S. B., and Walker R. J. (1995) Carius tube digestion for low-blank Rhenium–Osmium analysis. *Anal. Chem.* **67**(13), 2136–2141.

Shirey S. B., and Walker R. J. (1998) The Re–Os isotope system in cosmochemistry and high-temperature geochemistry. *Ann. Rev. Earth Planet. Sci.* **26**, 423–500.

Shukolyukov A. and Lugmair G. W. (2006) The Mn–Cr isotope systematics in the ureilites Kenna and LEW 85440. *Lunar Planet. Sci. Conf.* **37**. #1478 (abstr.) [CD-ROM].

Singletary S., and Grove T. L. (2003) Early petrologic processes on the ureilite parent body. *Meteorit. Planet. Sci.* **38**(1), 95–108.

Singletary S., and Grove T. L. (2006) Experimental constraints on ureilite petrogenesis. *Geochim. Cosmochim. Acta* **70**, 1291–1308.

Sinha S. K., Sack R. O., and Lipschutz M. E. (1997) Ureilite meteorites: equilibration temperatures and smelting reactions. *Geochim. Cosmochim. Acta* **61**(19), 4235–4242.

Smoliar M. I., Walker R. J., and Morgan J. W. (1996) Re–Os Ages of Group IIA, IIIA, IVA, and IVB iron meteorites. *Science* **271**(5252), 1099–1102.

Spitz A. H., and Boynton W. V. (1991) Trace element analysis of ureilites: new constraints on their petrogenesis. *Geochim. Cosmochim. Acta* **55**(11), 3417–3430.

Takeda H. (1987) A coexisting orthopyroxene-pigeonite pair in Yamato-791538 and formation condition of ureilites. *Meteoritics* **22**(4), 511–512.

Takeda H., Mori H., and Ogata H. (1989) Mineralogy of augite-bearing ureilites and the origin of their chemical trends. *Meteoritics* **24**(2), 73–81.

Torigoye-Kita N., Misawa K., and Tatsumoto M. (1995a) Reply to the comment by C.A. Goodrich, G.W. Lugmair, M.J. Drake, and P.J. Patchett on U–Th–Pb and Sm–Nd isotopic systematics of the Goalpara ureilite: resolution of terrestrial contamination. *Geochim. Cosmochim. Acta* **59**(19), 4087–4091.

Torigoye-Kita N., Misawa K., and Tatsumoto M. (1995b) U–Th–Pb and Sm–Nd isotopic systematics of the Goalpara ureilite: resolution of terrestrial contamination. *Geochim. Cosmochim. Acta* **59**(2), 381–390.

Torigoye-Kita N., Tatsumoto M., Meeker G. P., and Yanai K. (1995c) The 4.56 Ga U–Pb age of the MET 78008 ureilite. *Geochim. Cosmochim. Acta* **59**(11), 2319–2329.

Trinquier A., Birck J. L., and Allègre C. J. (2005) ^{54}Cr-anomalies in the solar system: their extent and origin. *Lunar & Planetary Science Conference* **36**. #1259 (abstr.) [CD-ROM].

Walker D., and Grove T. (1993) Ureilite smelting. *Meteoritics* **28**(5), 629–636.

Walker R. J., Horan M. F., Morgan J. W., Becker H., Grossman J. N., and Rubin A. E. (2002) Comparative 187Re-187Os systematics of chondrites: Implications regarding early solar system processes. *Geochim. Cosmochim. Acta* **66**(23), 4187–4201.

Wänke H., Baddenhausen H., Spettel B., Teschke F., Quijano-Rico M., Dreibus G., and Palme H. (1972) The chemistry of Haverö ureilite. *Meteoritics* **7**(4), 579–590.

Warren P. H., and Huber H. (2006) Ureilite petrogenesis: a limited role for smelting during anatexis and catastrophic disruption. *Meteorit. Planet. Sci.* **41**(6), 835–849.

Warren P. H., and Kallemeyn G. W. (1992) Explosive volcanism and the graphite-oxygen fugacity buffer on the parent asteroid(s) of the ureilite meteorites. *Icarus* **100**(1), 110–126.

Warren P. H., Ulff-Møller F., Huber H., and Kallemeyn G. W. (2006) Siderophile geochemistry of ureilites: a record of early stages of planetesimal core formation. *Geochim. Cosmochim. Acta* **70**(8), 2104–2126.

Wasson J. T., and Kallemeyn G. W. (1988) Compositions of chondrites. *Philos. Trans. R. Soc. Lond., A: Math. Phys. Sci.* **325**, 535–544.

Weisberg M. K., Prinz M., Clayton R. N., Mayeda T. K., Sugiura N., Zashu S., and Ebihara M. (2001) A new metal-rich chondrite grouplet. *Meteorit. Planet. Sci.* **36**, 401–418.

Wiik H. B. (1972) The chemical composition of the Havero meteorite and the genesis of ureilites. *Meteoritics* **7**, 553–557.

Wlotzka F. (1972) Haverö ureilite: Evidence for recrystallization and partial reduction. *Meteoritics* **7**(4), 591–600.

Wlotzka F. (1993) A weathering scale for the ordinary chondrites (abstr.). *Meteoritics* **28**(3), 460.

Yanai K., and Noda M. (2005) Petrological comparison of Mongolian Jalanash ureilite and twelve Antarctic ureilites. *Lunar Planet. Sci. Conf.* **36**. #1028 (abstr.) [CD-ROM].

Associate editor: Noriko Kita